UNIVERSITY OF BIRMINGHAM

Research at Birmingham

Heterogeneous reaction of N2O5 with airborne TiO2 particles and its implication for stratospheric particle injection

Tang, M. J.; Telford, P. J.; Pope, Francis; Rkiouak, L.; Abraham, N. L.; Archibald, A. T.; Braesicke, P.; Pyle, J. A.; Mcgregor, J.; Watson, I. M.; Cox, R. A.; Kalberer, M.

DOI:
10.5194/acp-14-6035-2014

Atmos. Chem. Phys., 14, 6035–6048, 2014
www.atmos-chem-phys.net/14/6035/2014/
doi:10.5194/acp-14-6035-2014

Atmospheric Chemistry and Physics
Open Access

Heterogeneous reaction of N_2O_5 with airborne TiO_2 particles and its implication for stratospheric particle injection

M. J. Tang[1,2], P. J. Telford[1,4], F. D. Pope[3], L. Rkiouak[1,5], N. L. Abraham[1,4], A. T. Archibald[1,4], P. Braesicke[1,4,*], J. A. Pyle[1,4], J. McGregor[6], I. M. Watson[2], R. A. Cox[1], and M. Kalberer[1]

[1]Department of Chemistry, University of Cambridge, Cambridge CB2 1EW, UK
[2]School of Earth Sciences, University of Bristol, Bristol BS8 1RJ, UK
[3]School of Geography, Earth and Environmental Sciences, University of Birmingham, Birmingham B15 2TT, UK
[4]National Centre for Atmospheric Science, NCAS, UK
[5]Department of Chemical Engineering and Biotechnology, University of Cambridge, Cambridge CB2 3RA, UK
[6]Department of Chemical and Biological Engineering, University of Sheffield, Sheffield S1 3JD, UK
[*]now at: IMK-ASF, Karlsruhe Institute of Technology, Karlsruhe, Germany

Correspondence to: M. Kalberer (markus.kalberer@atm.ch.cam.ac.uk)

Received: 28 January 2014 – Published in Atmos. Chem. Phys. Discuss.: 18 February 2014
Revised: 9 May 2014 – Accepted: 16 May 2014 – Published: 18 June 2014

Abstract. Injection of aerosol particles (or their precursors) into the stratosphere to scatter solar radiation back into space has been suggested as a solar-radiation management scheme for the mitigation of global warming. TiO_2 has recently been highlighted as a possible candidate particle because of its high refractive index, but its impact on stratospheric chemistry via heterogeneous reactions is as yet unknown. In this work the heterogeneous reaction of airborne submicrometre TiO_2 particles with N_2O_5 has been investigated for the first time, at room temperature and different relative humidities (RH), using an atmospheric pressure aerosol flow tube. The uptake coefficient of N_2O_5 onto TiO_2, $\gamma(N_2O_5)$, was determined to be $\sim 1.0 \times 10^{-3}$ at low RH, increasing to $\sim 3 \times 10^{-3}$ at 60 % RH. The uptake of N_2O_5 onto TiO_2 is then included in the UKCA chemistry–climate model to assess the impact of this reaction on stratospheric chemistry. While the impact of TiO_2 on the scattering of solar radiation is chosen to be similar to the aerosol from the Mt Pinatubo eruption, the impact of TiO_2 injection on stratospheric N_2O_5 is much smaller.

1 Introduction

Injection of aerosol particles (or their precursors) into the stratosphere to scatter solar radiation back into space has been suggested as a solar-radiation management (SRM) scheme for the mitigation of global warming due to the increasing concentrations of greenhouse gases (see, e.g., Shepherd, 2009). Most of the stratospheric particle injection research to date has focused on the use of sulfuric acid particles (Crutzen, 2006; Ferraro et al., 2011) because of their natural presence in the stratosphere (SPARC, 2006). During periods of low volcanic activity there is a background sulfate aerosol layer with a global loading of 0.65 ± 0.2 Tg (SPARC, 2006). However, after large explosive volcanic eruptions the concentration increases dramatically. For example, after the Mt Pinatubo eruption in the Philippines in 1991 it is estimated that at peak there was ~ 30 Tg H_2SO_4 in the stratosphere (Guo et al., 2004; McCormick et al., 1995). Several minerals, including TiO_2, have recently been suggested as possible alternative candidate particles to be injected into the stratosphere for SRM (Pope et al., 2012), due to their high light-scattering ability by virtue of a high refractive index. For instance, the refractive index at 550 nm is 2.5 for TiO_2 compared to 1.5 for the naturally occurring 70 wt % H_2SO_4 particles. The scattering ability of aerosol particles is also dependent upon the size of the particles. Assuming that the size

Published by Copernicus Publications on behalf of the European Geosciences Union.

can be optimized, it is estimated that, to achieve the same scattering effect, the use of TiO_2 for SRM requires a factor of ∼ 3 less in mass (and a factor of ∼ 7 less in volume) than that of H_2SO_4 aerosols, i.e. only 10 Tg TiO_2 particles are needed (Pope et al., 2012).

Stratospheric particle injection for SRM would increase the burden of stratospheric aerosols and thus also the surface area available for heterogeneous reactions. The production and/or removal of gas-phase species via heterogeneous reactions could perturb the stratospheric chemistry and impact the stratospheric O_3 level (Molina et al., 1996; Solomon, 1999; Tilmes et al., 2008). The eruption of Mt Pinatubo introduced an additional 30 Tg of aerosols into the stratosphere. This increased aerosol loading resulted in surface cooling and produced record low levels of stratospheric ozone (Dutton and Christy, 1992; McCormick et al., 1995).

While the heterogeneous reactions of sulfuric acid particles in the stratosphere are well characterized (Ammann et al., 2013; Sander et al., 2011), the heterogeneous reactivity of mineral surface towards stratospherically important trace gases has seldom been investigated (Crowley et al., 2010), and this impedes us from a reliable assessment of their impact on stratospheric chemistry and, more specifically, stratospheric O_3 (Pope et al., 2012). The heterogeneous reaction of N_2O_5 (Reaction R1), one of the most important heterogeneous reactions in the stratosphere, converts reactive nitrogen oxides (NO and NO_2), which are involved in catalytic cycles leading to stratospheric O_3 depletion, to non-reactive nitric acid (Solomon, 1999):

$$N_2O_5 + H_2O + \text{surface} \rightarrow 2HNO_3. \tag{R1}$$

It has been shown that after the eruption of Mt Pinatubo, the uptake of N_2O_5 onto sulfuric acid particles led to significant change in the partitioning of nitrogen species in the stratosphere (Fahey et al., 1993; Solomon, 1999).

Mineral dust particles are the most abundant aerosol particles in the troposphere on a mass basis (Huneeus et al., 2011; Textor et al., 2006). Tropospheric mineral dust aerosols have a large impact on direct and indirect radiative forcing (Balkanski et al., 2007; Cziczo et al., 2013), and their heterogeneous reactions with several trace gases can significantly influence tropospheric photochemistry (Dentener et al., 1996) and modify the composition of dust particles (Sullivan et al., 2007). TiO_2, an important component in natural mineral dust particles (Hanisch and Crowley, 2003; Usher et al., 2003), is of particular interest because heterogeneous reactivity towards some trace gases (e.g., NO_2, O_3) is significantly enhanced under illuminated conditions (Ndour et al., 2008; Nicolas et al., 2009). TiO_2 is also a well-established photocatalyst for a wide range of reactions (Linsebigler et al., 1995; Nakata and Fujishima, 2012), including the conversion of NO_x species (Bedjanian and El Zein, 2012; Ndour et al., 2008).

N_2O_5, mainly formed at night-time due to the reaction of NO_2 with NO_3 radicals (Wayne et al., 1991), is an important temporary reservoir for NO_x (NO + NO_2), and its uptake onto aerosol particles contributes to the removal of NO_x and the formation of particulate nitrate (Brown et al., 2006; Brown and Stutz, 2012), and the production of $ClNO_2$ (Phillips et al., 2012; Thornton et al., 2010), an important precursor of Cl atoms in the troposphere.

The kinetics of the uptake of N_2O_5 onto desert dust particles and their surrogates (e.g., Arizona Test Dust, illite) has been reported by several previous studies (Karagulian et al., 2006; Mogili et al., 2006; Seisel et al., 2005; Tang et al., 2010, 2012, 2014; Wagner et al., 2008, 2009). In addition, Seisel et al. (2005) observed the formation of nitrate on mineral dust particles due to the uptake of N_2O_5 using diffuse reflectance FTIR (Fourier transform infrared spectroscopy), and Tang et al. (2012) further confirmed that the yield of nitrate is ∼ 2 (as expected from Reaction R1) within the experimental uncertainty, and that the formation of NO_2 is negligible. However, to the best of our knowledge, the reaction of N_2O_5 with TiO_2 has never been studied. In this work an aerosol flow tube was deployed to investigate the kinetics of the heterogeneous reaction of N_2O_5 with airborne submicron TiO_2 particles at room temperature and at different relative humidities (RH). We note that in the lower stratosphere the typical temperature and RH ranges are 200–220 K and < 40 %, respectively (Dee et al., 2011). While our experimental work covers the RH range relevant for the stratosphere, it has been carried out at room temperature instead of ∼ 200 K due to experimental difficulties.

Telford et al. (2009) used the UKCA (United Kingdom Chemistry and Aerosol model) chemistry–climate model to attribute ozone changes due to volcanic aerosol after the Mt Pinatubo eruption in 1991. Here, we use a successor of this model to assess the effect of N_2O_5 uptake onto TiO_2 particles on the stratospheric composition. We construct a case study based on the eruption of Mt Pinatubo, comparing the effects of TiO_2 to those from the volcanic sulfate and to a situation with only background aerosol amounts present. The changes in reactive nitrogen species and ozone due to the heterogeneous reaction of TiO_2 with N_2O_5 are assessed relative to sulfate aerosol impacts.

2 Methodologies

2.1 Experimental section

A new atmospheric pressure aerosol flow tube was deployed to investigate the heterogeneous reaction of N_2O_5 with airborne TiO_2 particles. The schematic diagram of the aerosol flow tube is shown in Fig. 1. Since it is presented for the first time, a detailed description of the aerosol flow tube is given in this study. All experiments were carried out at 296 ± 2 K, and N_2 was used unless otherwise stated.

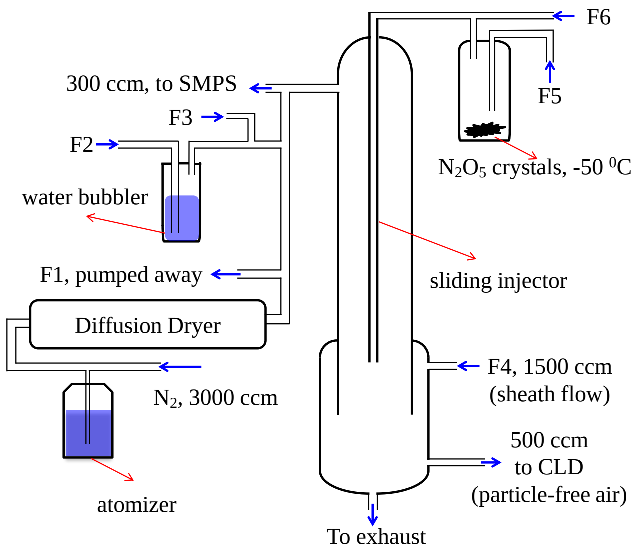

Figure 1. Schematic diagram of the aerosol flow tube. SMPS: scanning mobility particle sizer; CLD: chemiluminescence detector, used to measure the N_2O_5 concentration (measured as the change in the NO concentration). All the flows (except the flow applied to the atomizer) were controlled by mass flow controllers. Flow details are provided in text.

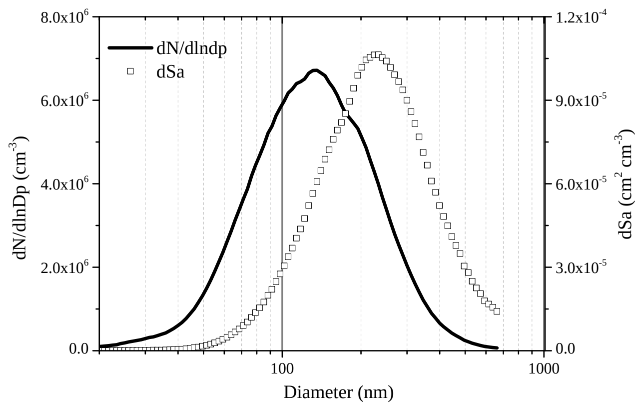

Figure 2. Typical number (left y axis) and surface (right y axis) size distribution (mobility diameter, measured by the SMPS) of TiO_2 aerosols used in this study.

2.1.1 Aerosol flow tube

The atmospheric-pressure aerosol flow tube (AFT) is a horizontal-mounted Pyrex tube with an inner diameter of 30 mm and a length of 100 cm. The total flow in the AFT was 1550 mL min^{-1} at 1 bar and room temperature, resulting in a linear flow velocity of 2.36 cm s^{-1}, a maximum residence time of ~40 s, and a Reynolds number of 46, i.e. the flow was laminar. The entrance length required to develop the laminar flow and the mixing length were calculated to be ~8 and ~13 cm, respectively (Keyser, 1984), using a diffusion coefficient of 0.085 cm^2 s^{-1} for N_2O_5 (Wagner et al., 2008). For all the experiments, only the middle part of the flow tube (30–80 cm) where the gases have been well mixed and the laminar flow has been fully developed was used to measure the uptake kinetics.

TiO_2 aerosols, after being adjusted to the desired RH, were introduced into the top of the AFT via the side arm, and N_2O_5 was delivered into the centre of the flow tube via a stainless-steel injector. The position of the stainless-steel sliding injector (outer diameter: 6 mm) could be adjusted to vary the interaction time of N_2O_5 with airborne TiO_2 particles. The inner wall of the AFT was coated with an inert FEP (United Kingdom Chemistry and Aerosol model) film to reduce the loss of gaseous N_2O_5 onto the wall. The RH and the total flow rate in the flow tube were measured both before and after each experiment.

2.1.2 Aerosol generation and characterization

TiO_2 aerosols were generated by atomizing a P25 TiO_2–water suspension (with a TiO_2 mass fraction of 1–2 %) with ~3 bar N_2 using a commercial constant output atomizer (Model 3076, TSI, USA). The TiO_2–water suspension was constantly stirred using a magnetic stirrer, in order to keep the suspension homogeneous so that the generated aerosol would have a constant number concentration and stable size distribution. The resulting aerosol flow (~3000 mL min^{-1}) was delivered through 1–3 (depending on the desired RH in the flow tube) diffusion dryers in series. The aerosol flow then passed through a Berner cascade impactor (not shown in Fig. 1) with a cut-off size of 1 µm at a flow rate of 3000 mL min^{-1}, in order to remove super-micrometre particles perform the wall loss measurement. A fraction of the aerosol flow was then pumped away (F1). The remaining aerosol flow either was delivered through a filter (not shown in Fig. 1) to remove all the particles or, alternatively, the filter could also be bypassed. The aerosol flow was conditioned to desired RH and diluted to a total flow of 1800 mL min^{-1} (by F2 and F3, as shown in Fig. 1). After that, 300 mL min^{-1} of the aerosol flow was sampled into a scanning mobility particle sizer (SMPS) to measure the number concentration and size distribution, and the remaining 1500 mL min^{-1} flow was delivered into the aerosol flow tube via the side arm. Metal (outer diameter: 0.25″) or conductive silicone (TSI, inner diameter: 0.19″) tubing was used to deliver aerosols, in order to minimize the loss of TiO_2 particles during transport.

An SMPS was used to characterize the number concentration and size distribution of TiO_2 aerosol particles online. It consists of a differential mobility analyser (TSI 3081), and a condensation particle counter (CPC, TSI 3775) which was operated at a sampling flow rate of 300 mL min^{-1}. The sheath flow in the DMA was set to 3000 mL min^{-1}, resulting in a detectable mobility size range of 14–672 nm. The time resolution of the SMPS measurement is 150 s. The measured number concentration and size distribution were quite stable, and the variation of aerosol surface area concentration is typically < 5 % during each experiment (typically ∼ 60–80 min), as shown in Table 1. A typical size distribution of TiO_2 aerosols used in this study is shown in Fig. 2, suggesting that the contribution of undetected larger particles (with mobility diameters > 672 nm) to the total surface area concentration is negligible. For TiO_2 aerosols used in this work, $dN/d\ln d$ maximizes around 150 nm, and the average surface area of one TiO_2 particle is $\sim 9.0 \times 10^{-10}$ cm^2. The mobility diameters measured by the SMPS are used to calculate the surface area, which is then used to calculate the uptake coefficient, though we note that TiO_2 particles used in this work are non-spherical and thus the mobility-diameter-based surface area can be different from the true surface area. The BET surface area was determined to be 8.3 m^2 g^{-1}, ∼ 60% larger than the mobility-diameter-based surface area, i.e. ∼ 5.7 m^2 g^{-1}.

2.1.3 N_2O_5 generation

Crystalline N_2O_5 was synthesized by mixing a small flow of pure NO with 500 mL min^{-1} O_3 / O_2 in a glass reactor and trapping the product at −78 °C using a cold finger immersed in an ethanol-dry ice bath. O_3 was generated by electrical discharge of O_2 which has been delivered through a P_2O_5–silica gel scrubber to remove any residual water vapour before entering the electrical discharger. After mixing NO with O_3 / O_2 in the glass reactor, brown colour appeared initially, indicating the formation of NO_2 (Reaction R2). The brown colour mostly disappeared at the end of the reactor, suggesting that most of the NO_2 was converted to N_2O_5 (Reactions R3–R4a):

$$NO + O_3 \rightarrow NO_2 + O_2, \quad \text{(R2)}$$

$$NO_2 + O_3 \rightarrow NO_3 + O_2, \quad \text{(R3)}$$

$$NO_2 + NO_3 + M \rightarrow N_2O_5 + M. \quad \text{(R4a)}$$

The synthesised N_2O_5 crystals were stored in an ethanol bath kept at −50 °C using a cryostat. In order to further purify the N_2O_5 sample, the following procedure was repeated a few times after the cryostat was warmed to −20 °C: (i) the cold finger was connected to the vacuum line; (ii) the cold finger was disconnected from the vacuum line (by shutting the valve) and the cold finger was filled with dry N_2 (which was passed through a P_2O_5–silica gel scrubber) to ∼ 1 bar; (iii) the cold finger was disconnected from the dry N_2 flow, and then connected to the vacuum line. This procedure was found to largely reduce the NO_2 impurity which was not completely oxidized by O_3 and thus also trapped in the cold finger at −76 °C during the N_2O_5 synthesis. A small N_2 flow (F5 in Fig. 1, usually 5–10 mL min^{-1}) was passed through a P_2O_5–silica scrubber (to remove any residual water vapour) and then used to elute gaseous N_2O_5 from the crystalline sample. The resulting N_2O_5 flow was diluted by another N_2 flow (F6) to a total flow of 50 mL min^{-1} and then delivered into the centre of the aerosol flow tube through a 1/8″ Teflon tube in the sliding injector.

2.1.4 N_2O_5 detection

The bottom 30 cm of the AFT was coaxially inserted into another FEP-coated Pyrex tube with a length of 60 cm and an inner diameter of 43 mm. A sheath flow of 1500 mL min^{-1} (F4) was fed into the annular space between the two coaxial Pyrex tubes. The aerosol flow in the flow tube had the same linear flow velocity as the sheath flow in order to minimize the turbulence when they were mixed at the end of the AFT. Gases, including N_2O_5, could exchange between the sheath flow and the aerosol flow because their diffusion coefficients are around 0.1 cm^2 s^{-1}, while airborne particles remain in the centre due to their very small diffusion coefficients (10^{-7}–10^{-6} cm^2 s^{-1}; Hinds, 1996). At the end of the larger Pyrex tube, ∼ 500 mL min^{-1} was sampled through a 1/4″ Teflon tube which intruded 1–2 mm into the inner wall of the larger tube. The sampled flow was checked by a CPC, and the measured particle number concentration was less than 10 cm^{-3} even when the number concentration of the TiO_2 aerosols in the AFT reached $\sim 1 \times 10^7$ particles cm^{-3}. This novel gas–particle separation method in the aerosol flow tube study was first presented by Rouviere et al. (2010), and the current design was previously described by Tang et al. (2012).

The 500 mL min^{-1} particle-free air sampled from the AFT was mixed with a small flow (∼ 5 mL min^{-1}, controlled by a mass flow controller) of NO (100 ppmv in N_2) and then delivered into a glass reactor which was heated to 100 °C. N_2O_5 was thermally decomposed to NO_2 and NO_3 radicals (Reaction R4b), which was then titrated by NO to form NO_2 (Reaction R5):

$$N_2O_5 + M \rightarrow NO_2 + NO_3 + M, \quad \text{(R4b)}$$

$$NO_3 + NO \rightarrow NO_2 + NO_2. \quad \text{(R5)}$$

The change in NO concentration is equal to the N_2O_5 concentration. The glass reactor used in this work has a volume of ∼ 30 cm^3 (with a length of 10 cm and an inner diameter of 2 cm), leading to a residence time of ∼ 3 s at a flow rate of ∼ 500 mL min^{-1}. At atmospheric pressure and 90 °C, the lifetime of N_2O_5 with respect to thermal decomposition (Reaction R4b) is around ∼ 0.05 s and the lifetime of NO_3 radicals due to the titration by 1 ppmv NO (Reaction R5) is ∼ 0.002 s, as detailed by Wagner et al. (2008). The residence time in the reactor is much longer than the lifetime of N_2O_5 and NO_3 under our experimental condition, ensuring that all the N_2O_5 should be decomposed and then titrated by NO. This scheme has been suggested as an absolute method to calibrate other N_2O_5 detection methods (e.g., CIMS) (Fahey et al., 1985), and is also widely used to study the heterogeneous reactions of N_2O_5 with aerosol particles (e.g., Wagner et al., 2008).

The NO concentration was measured by a chemiluminescence-based nitrogen oxides analyser (Model

Table 1. Loss rate of N_2O_5 on TiO_2 (k_a), total surface area of TiO_2 particles in the flow tube (S_a) and uptake coefficients of N_2O_5 onto TiO_2 aerosols, $\gamma(N_2O_5)$, at different relative humidities. All the errors shown here are 1σ statistically.

RH (%)	k_a ($\times 10^{-2}$ s^{-1})	S_a ($\times 10^{-3}$ cm^2 cm^{-3})	$\gamma(N_2O_5)$ ($\times 10^{-3}$)	average $\gamma(N_2O_5)$ ($\times 10^{-3}$)
5 ± 1	3.02 ± 1.62	4.39 ± 0.26	1.15 ± 0.62	1.22 ± 0.21
	2.64 ± 0.58	3.79 ± 0.06	1.16 ± 0.26	
	2.44 ± 1.11	3.02 ± 0.10	1.35 ± 0.61	
12 ± 2	2.39 ± 0.40	2.75 ± 0.16	1.45 ± 0.24	1.34 ± 0.18
	2.86 ± 0.36	3.80 ± 0.52	1.26 ± 0.16	
	2.65 ± 0.22	2.89 ± 0.33	1.53 ± 0.13	
	1.84 ± 0.24	2.70 ± 0.14	1.14 ± 0.15	
23 ± 2	6.26 ± 0.20	1.75 ± 0.17	0.60 ± 0.19	0.68 ± 0.13
	2.27 ± 0.28	4.89 ± 0.21	0.77 ± 0.01	
33 ± 2	1.00 ± 0.37	2.27 ± 0.16	0.73 ± 0.27	0.86 ± 0.17
	1.27 ± 0.30	2.01 ± 0.12	1.06 ± 0.25	
	1.07 ± 0.26	2.23 ± 0.09	0.80 ± 0.20	
45 ± 3	1.29 ± 0.26	1.59 ± 0.33	1.36 ± 0.27	1.52 ± 0.34
	2.53 ± 0.60	3.00 ± 0.05	1.41 ± 0.31	
	2.91 ± 0.56	2.86 ± 0.05	1.70 ± 0.33	
	2.66 ± 0.58	2.75 ± 0.02	1.62 ± 0.35	
60 ± 3	5.22 ± 1.40	2.86 ± 0.06	3.08 ± 0.82	2.98 ± 1.36
	3.84 ± 1.04	2.24 ± 0.09	2.89 ± 0.78	

200E, Teledyne Instruments, USA), which has a sampling flow rate of 500 mL min^{-1} ($\pm$10 %) and a detection limit of $\sim$0.5 ppbv with a time resolution of 1 min. The NO measurement was calibrated using a certificated NO standard. The initial N_2O_5 mixing ratios used in in the flow tube were in the range of 1–2 ppmv.

2.1.5 Chemicals

Pure NO (with a purity of > 99 %) in a lecture bottle and the 100 ppmv NO in N_2 (with actual mixing ratio within $\pm$1 % deviated from the stated value) were both supplied by CK Gas (UK). N_2 and O_2 were provided by BOC Industrial Gases (UK). P25 TiO_2 particles were purchased from Degussa-Hüls AG (Germany) as dry powder, and have an anatase to rutile ratio of 3 : 1.

2.2 Model description

The UKCA chemistry–climate model in its whole atmosphere configuration (Braesicke et al., 2014; Telford et al., 2014) was used to simulate the effects of the heterogeneous reaction of TiO_2 with N_2O_5 in the stratosphere. This is a relatively new configuration that combines the well-established tropospheric (O'Connor et al., 2014) and stratospheric (Morgenstern et al., 2009) versions of the model. It includes the O_x, HO_x, and NO_x chemical cycles and the oxidation of CO, ethane, propane, and isoprene in addition to chlorine and bromine chemistry including heterogeneous processes on polar stratospheric clouds (PSCs) and liquid sulfate aerosols.

We adopt an approach based on our previous study of the effects of the Pinatubo eruption on stratospheric ozone (Telford et al., 2009). Telford et al. (2009) used the UKCA model in a "nudged" configuration to constrain the dynamics of the model to observations (Telford et al., 2008, 2013), and examined the differences in ozone between scenarios with and without stratospheric sulfate aerosol caused by the Mt Pinatubo eruption. Here we consider a further scenario in which we introduce raised levels of TiO_2 into the stratosphere.

It has been suggested that in order to achieve the same solar radiation scattering effect as the eruption of Mt Pinatubo, 10 Tg TiO_2 aerosol particles with an assumed radius of 70 nm are needed (Pope et al., 2012). The total mass of TiO_2 particles (10 Tg) is converted to the total surface area, based on the known density (4.23 g cm^{-3}) and radius (70 nm). In the model the global distribution of the surface area concentration of TiO_2 aerosol is derived from that of the Pinatubo aerosol, scaling to take account of differences in the global mass, particle size, and density. The sulfate aerosol surface area concentration was derived from the SPARC climatology (SPARC, 2006). We perform two simulations for the TiO_2 scenario in which the uptake of N_2O_5 onto TiO_2 aerosols is included using two different uptake coefficients, i.e. 0.001 and 0.005, respectively. The two uptake coefficients used in the model are constrained by the experimental measurements, as detailed in Sect. 3. We compare these with a simulation with aerosols set to a background level and with a simulation with volcanically induced sulfate aerosols present. The 1990 stratospheric aerosol loading is chosen to represent the background condition (Telford et al., 2009). We examine the results over the course of 1992, as the effects of the eruption on the stratospheric chemistry were largest then, caused by the spread of the aerosols towards the poles (e.g., Telford et al., 2009). In our approach the loading of both sulfate and TiO_2 is then smaller than their peak loading. This contrasts with some of the figures given in Pope et al. (2012) that concentrate on a time horizon soon after the eruption when the radiative effect was greatest.

3 Results & discussion

3.1 Uptake kinetics

The decay of N_2O_5 in the aerosol flow tube is due to the removal of N_2O_5 by the wall and its uptake onto the aerosol surface. Under pseudo-first-order conditions, e.g., the number of reactive sites is in great excess of the gaseous reactant and hence does not change significantly during the trace gas–particle interaction time, the loss of N_2O_5 in the aerosol flow tube can be described as

$$[N_2O_5]_t = [N_2O_5]_0 \cdot \exp[-(k_w + k_a) \cdot t], \tag{1}$$

where $[N_2O_5]_t$ and $[N_2O_5]_0$ are the measured N_2O_5 concentrations at reaction times of t and 0, and k_w and k_a are the pseudo-first-order loss rates (s^{-1}) of N_2O_5 onto the flow tube wall and the aerosol surface, respectively. In a typical experiment, the total loss rate, $k_w + k_a$, was determined by measuring the N_2O_5 concentrations at five different injection positions (corresponding to five different reaction times) with TiO_2 aerosols present in the flow tube. Before and after measuring the total loss rate, the wall loss rate, k_w, was determined in a similar way, except passing the aerosol flow through a filter to remove all the TiO_2 particles before it was delivered into the flow tube via the side arm. The difference of k_w measured before and after introducing TiO_2 aerosols in the AFT was within the experimental uncertainty associated with k_w determination, indicating that the N_2O_5 wall loss did not change significantly during the uptake experiment.

A typical data set of the measured N_2O_5 mixing ratios at five different injection positions with and without TiO_2 aerosols present in the flow tube is shown in Fig. 3. The measured N_2O_5 loss rate with TiO_2 aerosols present in the AFT was significantly larger than that of the experiments without TiO_2 aerosols, and the difference is equal to k_a, the loss rate of N_2O_5 onto the aerosol surface. The direct derivation of loss rates from exponential decays (e.g., Fig. 3) assumes the plug flow condition and no radical/axial diffusion. However, under laminar flow conditions the flow is non-plug and axial and radical diffusion also contribute to the apparent (or experimentally derived) loss of N_2O_5; therefore, the true loss rate is different from the apparent loss rate. This effect on the apparent k_a can be corrected using the method described by (Brown, 1978) and is widely used in aerosol flow tube studies (e.g., Thornton et al., 2003). The effect is small, with the corrected k_a only < 5 % larger than the measured value. The rate of a heterogeneous reaction is usually described by the uptake coefficient, γ, which is equal to the probability that a gas molecule which collides with the surface is removed from the gas phase. The pseudo-first-order loss rate of N_2O_5 onto TiO_2 aerosol surface in the flow tube (after being corrected for the non-plug flow effect, etc.), k_a, is related to the uptake coefficient of N_2O_5 onto TiO_2 particles by Eq. (2) (Crowley et al., 2010):

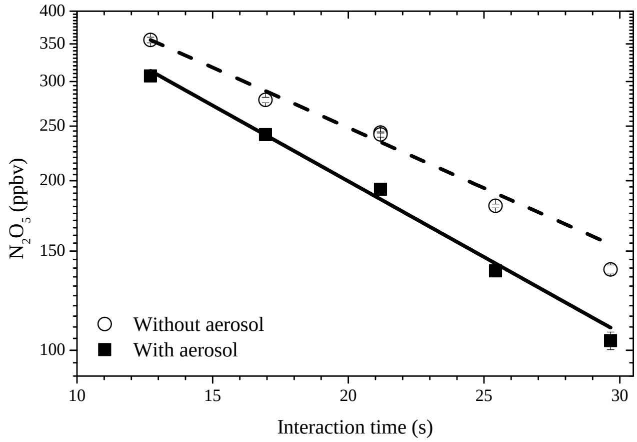

Figure 3. Measured N_2O_5 mixing ratios at different N_2O_5–TiO_2 interaction times, i.e. at different injection positions, with (solid squares) and without (open circles) TiO_2 aerosols in the flow tube. The pseudo-first-order decay rates of N_2O_5 are 0.0493 ± 0.0025 and $0.0619 \pm 0.0030\,s^{-1}$ without and with TiO_2 aerosols in the flow tube, respectively.

$$k_a = 0.25 \cdot \gamma_{exp}(N_2O_5) \cdot c(N_2O_5) \cdot S_a, \tag{2}$$

where $\gamma_{exp}(N_2O_5)$ is the measured (also called effective) uptake coefficient of N_2O_5, $c(N_2O_5)$ is the average molecular speed of N_2O_5 (24 096 cm s^{-1} at 296 K; Houston, 2001), and S_a is the surface area concentration ($cm^2\,cm^{-3}$) of TiO_2 aerosol in the flow tube.

As shown in Table 1 for each RH 2–4 repeat experiments were performed and Eq. (2) was used to derive the uptake coefficient for each experiment. The surface area concentration of TiO_2 aerosols was varied by a factor of about 2. The uptake coefficients of N_2O_5 onto TiO_2 particles are quite small ($< 3 \times 10^{-3}$), and very high aerosol concentrations (up to $4 \times 10^6\,cm^{-3}$) were needed to achieve a significant decay of N_2O_5 due to the heterogeneous reaction with TiO_2 particles. Thus, it was not possible to vary S_a over a broad enough range to determine $\gamma(N_2O_5)$ via the slope of a linear fit of k_a vs. S_a, equal to $0.25 \cdot \gamma(N_2O_5) \cdot c(N_2O_5)$, as has been done in previous studies (McNeill et al., 2006; Thornton et al., 2003).

A gradient of the N_2O_5 concentration close to the particle surface is formed due to the uptake of N_2O_5 onto the particle surface, leading to the decrease of effective uptake coefficient, $\gamma_{exp}(N_2O_5)$, compared to the true uptake coefficient, $\gamma(N_2O_5)$. This effect can be corrected by using the Fuchs–Stuggin equation (Fuchs and Sutugin, 1970; Pöschl et al., 2007):

$$\frac{1}{\gamma(N_2O_5)} = \frac{1}{\gamma_{exp}(N_2O_5)} - \frac{0.75 + 0.286\,Kn}{Kn \cdot (Kn+1)}, \quad (3)$$

where Kn is the Knudsen number. For mono-dispersed aerosol particles, Kn given by

$$Kn = \frac{6D(N_2O_5)}{c(N_2O_5) \cdot d}, \quad (4)$$

where $D(N_2O_5)$ is the diffusion coefficient of N_2O_5 ($0.085\,cm^2\,s^{-1}$ at 1 atm and 296 K; Wagner et al., 2008) and d is the diameter of the particle (cm), which is assumed to be the mobility diameter measured by the SMPS. For poly-dispersed aerosol particles, e.g., TiO_2 particles used in this work, Kn can be calculated by

$$Kn = \frac{\sum[Kn(i) \cdot N(i)]}{\sum N(i)} = \frac{6D(N_2O_5)}{c(N_2O_5)} \cdot \frac{\sum[N(i)/d_i]}{\sum N(i)}, \quad (5)$$

where *Kn(i)* and $N(i)$ is the Knudsen number and number concentration of particles in the ith bin with a diameter of d_i, respectively. The advantage of using Eq. (5) to calculate the Knudsen number for poly-dispersed aerosol particles is detailed by Tang et al. (2012). $\gamma(N_2O_5)$ is found to be only $\leq 2\,\%$ larger than $\gamma_{exp}(N_2O_5)$. The small difference between $\gamma(N_2O_5)$ and $\gamma_{exp}(N_2O_5)$ is due to the small (submicrometre) particle size used in this study and the relatively small uptake coefficient of N_2O_5 onto TiO_2 particles (as shown in Table 1). The recombination of NO_2 with NO_3 (Reaction R4a) leads to the formation of additional N_2O_5, and the removal of NO_3 by the aerosol and wall surface causes further removal of N_2O_5 (Reaction R4b). Wagner et al. (2008) and Tang et al. (2010) simulated the effects of these reactions on N_2O_5 uptake measurement, and concluded that at room temperature the influence is negligible.

3.2 Effects of relative humidity

The heterogeneous reaction of N_2O_5 with airborne TiO_2 particles was studied at six different relative humidities from ∼ 5 to 60 %. The results are summarized together with key experimental parameters in Table 1, and in Fig. 4 $\gamma(N_2O_5)$ is plotted as a function of RH. As shown in Fig. 4, $\gamma(N_2O_5)$ does not vary significantly with RH below 45 %.

An increase of $\gamma(N_2O_5)$, by a factor of 2–3, was observed when RH increased from 45 to 60 %. The water adsorption isotherm onto TiO_2 particles at 296 K, reported by Goodman et al. (2001), is also plotted in Fig. 4 (red curve, right y axis). It is interesting to note that the increase of $\gamma(N_2O_5)$ when RH increases above 45 % concurs with the onset of multilayers of adsorbed water on TiO_2 particles. It is well known that the heterogeneous uptake of N_2O_5 onto particles (including but not limited to minerals) is driven by the solvation of N_2O_5 (after being accommodated onto the surface) into liquid or adsorbed water in the particles, followed by its hydrolysis to form HNO_3 (Bertram and Thornton, 2009; Griffiths et al., 2009; Tang et al., 2012). The formation of multilayers of adsorbed water on the TiO_2 surface can promote the solvation and hydrolysis of N_2O_5 onto the surface, and thus increase the uptake coefficient of N_2O_5. Previous studies have also revealed that the formation of multilayers of adsorbed water at around 50 % RH has a significant impact of the uptake processes of other trace gases onto TiO_2 surface. For example, $\gamma(H_2O_2)$ onto TiO_2 particles decreases with increasing RH for RH below 40 %, but a further increase in RH does not cause any change of the uptake coefficient of H_2O_2 (Pradhan et al., 2010). γ(HCHO) onto TiO_2 particles under irradiated conditions (340–420 nm) increases with RH when RH is below 40 %, and a further increase in RH causes the reduction of γ(HCHO) (Sassine et al., 2010).

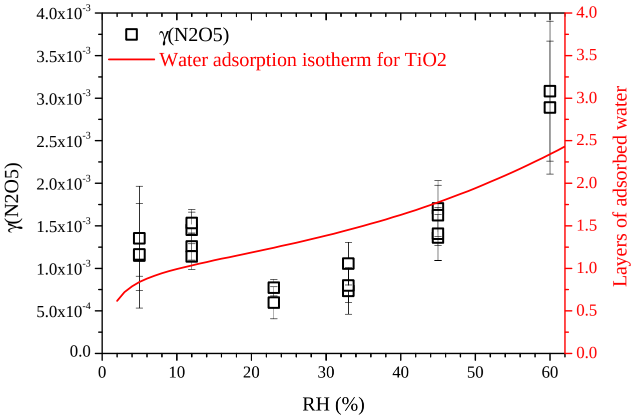

Figure 4. Uptake coefficients of N_2O_5 onto airborne TiO_2 particles (black squares, left x axis) at different relative humidities. The number of layers of the adsorbed water on TiO_2 particles (red curve, right y axis) at 296 K, measured by transmission FTIR spectroscopy (Goodman et al., 2001), is also plotted as a function of RH.

A close inspection of Fig. 4 further suggests that $\gamma(N_2O_5)$ may decrease with increasing RH between 5 and 20 % RH and reaches a minimum around 20 % RH, and above that $\gamma(N_2O_5)$ starts to increase with RH. The heterogeneous uptake of N_2O_5 onto mineral surfaces is suggested to proceed with two pathways: the reaction of N_2O_5 with surface OH groups or the heterogeneous hydrolysis of N_2O_5 by surface-adsorbed water, whereas the reaction with surface OH groups is faster (Seisel et al., 2005; Tang et al., 2014). FTIR observations showed that surface OH groups on Saharan dust particles were depleted during the exposure to N_2O_5, leading to the decrease of $\gamma(N_2O_5)$ with reaction time (Seisel et al., 2005). The uptake coefficient of N_2O_5 onto illite was found to decrease with increasing RH, and this is suggested to be due to the coverage of OH groups by adsorbed water at high RH (Tang et al., 2014). The minimum of $\gamma(N_2O_5)$ onto TiO_2 at 20 % RH may indicate that the increase of RH up to 20 % could cause the more reactive surface OH groups to be covered by surface-adsorbed water, while further increase in RH will promote the heterogeneous hydrolysis of N_2O_5 by surface-adsorbed water, i.e. the overall effect of the two competing roles of surface-adsorbed water results in a minimum of $\gamma(N_2O_5)$ at $\sim$20 % RH. The surface coverage of water is determined by RH, and is probably also affected by temperature. However, the RH-dependent water surface coverage has only been investigated at room temperature but not under lower stratospheric conditions (200–220 K).

3.3 Comparison with other relevant surfaces

TiO_2 is an important component in tropospheric mineral dust aerosols, and this work is the first time that the heterogeneous reaction of N_2O_5 with TiO_2 aerosols has been investigated. It is interesting to compare $\gamma(N_2O_5)$ onto TiO_2 particles with that onto other mineral dust particles. Only results reported by aerosol flow tube studies are compared here. Real desert dust and clay minerals show much higher heterogeneous reactivity towards N_2O_5: the uptake coefficient of N_2O_5, $\gamma(N_2O_5)$, is (1–2) $\times 10^{-2}$ for Saharan dust (Tang et al., 2012; Wagner et al., 2008), and (4–9) $\times 10^{-2}$ for illite (Tang et al., 2014), explained by the high density of OH groups in illite (Hatch et al., 2011). $\gamma(N_2O_5)$ was reported to be (4.5–8.6) $\times 10^{-3}$ for SiO_2 (Wagner et al., 2008) and (5–10) $\times 10^{-3}$ for Arizona Test Dust (Wagner et al., 2008; Tang et al., 2014), whose main components are SiO_2 and feldspar (Broadley et al., 2012), and the lower heterogeneous reactivity of SiO_2 and Arizona Test Dust towards N_2O_5 is mainly attributed to the low amount of surface-adsorbed water on the surface of the two particles, compared to clay and Saharan dust. The reactivity of $CaCO_3$ with N_2O_5 is very low at 0 % RH with $\gamma(N_2O_5)$ of $\sim 5 \times 10^{-3}$ but increases quickly with RH with $\gamma(N_2O_5)$ of $\sim 2 \times 10^{-2}$ at 71 % (Wagner et al., 2009). This is explained by the formation of $Ca(OH)(CO_3H)$ which might be highly reactive towards acidic trace gases (Al-Hosney and Grassian, 2005) at high RH.

The major motivation of this work is to provide kinetic data required to assess the impact on stratospheric N_2O_5, reactive nitrogen species, and O_3, if TiO_2 particles were injected into the lower stratosphere to scatter solar radiation back into space as a geoengineering scheme (Pope et al., 2012). Several types of particles – e.g., sulfuric acid, nitric acid trihydrate (NAT), and ice particles, are naturally present in the stratosphere (Solomon, 1999), and their heterogeneous reactivity towards N_2O_5 has been well characterized (Ammann et al., 2013; Crowley et al., 2010; Sander et al., 2011). The heterogeneous reaction of N_2O_5 with sulfuric acid has been investigated over a broad temperature range ($\sim$210–300 K), due to its importance in both stratosphere (Solomon, 1999) and troposphere (Dentener and Crutzen, 1993). $\gamma(N_2O_5)$ onto sulfuric acid particles increases with temperature, maximizes at $\sim$230 K, and then decreases with temperature (Ammann et al., 2013). The non-monotonic change of $\gamma(N_2O_5)$ as a function of temperature is caused by the combination of two processes: the positive temperature-dependent bulk reaction and the negative temperature-dependent accommodation/adsorption onto the surface. The overall temperature effect is small, and $\gamma(N_2O_5)$ onto sulfuric acid particles only changes by a factor of $\sim$3 when temperature is varied from 210 to 300 K. The heterogeneous reaction of N_2O_5 with TiO_2 particles was investigated only at room temperature ($\sim$296 K) in this work, due to the experimental challenges to measure $\gamma(N_2O_5)$ onto aerosol particles at stratospherically relevant temperatures ($\sim$200 K), and no previous studies have investigated the effect of temperature on the heterogeneous reaction of N_2O_5 with minerals. The weak dependence of $\gamma(N_2O_5)$ onto sulfuric acid particles on temperature leads us to believe that $\gamma(N_2O_5)$ onto TiO_2 particles under typical lower stratosphere conditions (temperature: 200–220 K; RH: < 40 %) (Dee et al., 2011) should not be larger than a factor of 5 compared to that at room temperature, i.e. $< 5 \times 10^{-3}$.

Stratospheric ice particles, an important component in polar stratospheric clouds (PSCs), show significant reactivity towards N_2O_5, with $\gamma(N_2O_5)$ of 0.02 at 190–200 K (Crowley et al., 2010), and the reactivity of NAT, another important type of particles in PSCs, is much lower, with $\gamma(N_2O_5)$ of around $\sim 6 \times 10^{-4}$ at 190–200 K (Hanson and Ravishankara, 1991). In addition, a $\gamma(N_2O_5)$ of $\sim 6.5 \times 10^{-3}$ was measured for sulfuric acid tetrahydrate (SAT) and ranges from 4×10^{-4} to 1.65×10^{-3} (RH dependent) for sulfuric acid monohydrate (SAM) (Crowley et al., 2010).

To summarize, under the conditions investigated P25 TiO_2 particles show much lower reactivity towards N_2O_5 than sulfuric acid and ice particles and significantly higher reactivity than NAT, and their reactivity towards N_2O_5 is of the same order of magnitude as SAT and SAM.

3.4 Implication for stratospheric particle injection

The impact of N_2O_5 uptake onto TiO_2 aerosols on the stratospheric trace gas composition is assessed using the UKCA model. Two values of $\gamma(N_2O_5)$ onto TiO_2 aerosol particles were used in the model. The first one is 0.001, equal to the experimentally determined uptake coefficient at room temperature and low relative humidity. The second one is 0.005, which we believe represents the upper limit of $\gamma(N_2O_5)$ onto TiO_2 aerosol particles under typical stratospheric conditions, taking into account the uncertainties associated with temperature (typically 200–220 K) and relative humidities (typically 0–40 %) (Pope et al., 2012).

We note that, at the present at least, the impact of stratospheric aerosols on trace gases is dominated by chlorine activation (Solomon, 1999). Thus, to fully assess the impact of TiO_2, especially on ozone, these further reactions need to be taken into account. However, we can gain an understanding of the relative effect of TiO_2 compared to sulfuric acid by considering its effect on N_2O_5. We also acknowledge that by choosing to constrain the dynamical changes to those observed after the eruption of Mt Pinatubo, whilst allowing us to focus on the changes in heterogeneous chemistry, we neglect differences in the dynamical response and their feedbacks onto the chemistry. The effects of stratospheric aerosols, including TiO_2, on stratospheric dynamics have been considered elsewhere (Pope et al., 2012), and we consider it is worthwhile exploring the impacts of heterogeneous chemistry in isolation before constructing case studies with a more elaborate set of feedbacks.

The surface area density of the additional sulfate (i.e. after the Mt Pinatubo eruption) and TiO_2 aerosols is shown in Fig. 5. The lower mass loading, higher density, and larger particle size of the TiO_2 particles all contribute to the much lower surface aerosol density of the TiO_2 aerosol compared to the Pinatubo sulfate aerosol. The higher density of TiO_2 and lower projected mass are the main drivers of the decreases in the surface area density. Although our assumption of completely uniform particle size is not realistic, it allows to assess the effects of N_2O_5 under idealized conditions.

Figure 6 shows the effects of these extra aerosols on the simulated N_2O_5 averaged over 1992. The run with Pinatubo aerosols has lost almost all N_2O_5 in the lower stratosphere, around 90 %, compared to the base run. The reductions with the addition of the TiO_2 aerosols are much smaller, around 20–30 % in much of the lower stratosphere using the higher uptake coefficient (0.005), and only ∼ 10 % using the lower value (0.001). One region where there is slightly greater depletion is over Antarctica, and this may be a result of overestimating surface area densities over the poles where we have no observational data constraint. Overall the effects of our simulated TiO_2 in the stratosphere are considerably lower than the effects of the Pinatubo eruption.

The impacts on ozone are also examined. As in previous model studies (Telford et al., 2009) we found the volcanic sulfate aerosols caused large decreases in ozone (up to 10 % in the northern extra-tropics) in the lower stratosphere caused by increased Cl activation, and small increases (2–3 %) at higher altitudes, driven by decreases in NO_x. As we do not include any Cl activation on the TiO_2 aerosols we do not see the same lower stratospheric decreases, but do simulate ozone increases through most of the stratosphere, peaking at around 2.5 % at 35 km linked to decreases in NO_x for both TiO_2 runs. This increase in ozone has an impact on the troposphere, lowering photolysis rates contributing to increases in tropospheric values of N_2O_5, as seen in Fig. 6.

Whilst we acknowledge that there are limitations to these simulations, most notably the inclusion of only a single heterogeneous process on the TiO_2, but also due to factors such as the omission of the TiO_2 aerosols from the photolysis calculation, we believe the qualitative conclusions from them are valid. We base this on our understanding of the atmospheric response to the eruption of Mt Pinatubo. Here the dominant factor on the global stratospheric chemistry was the increased heterogeneous chemistry, with factors such as changes in photolysis rates being secondary. However, further studies are required on effects of photolysis change in photolysis before any definite conclusions can be reached.

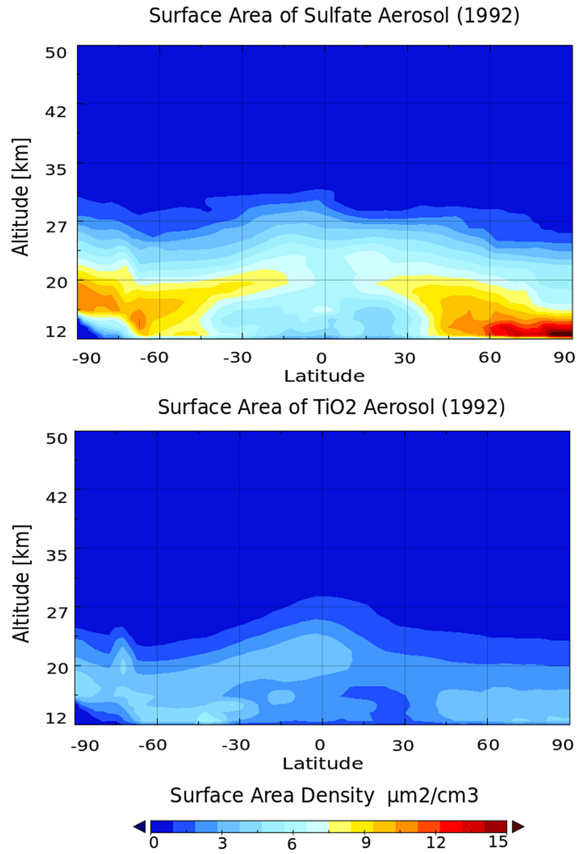

Figure 5. Surface area density ($\mu m^2\ cm^{-3}$) of sulfate particles after the Mt Pinatubo eruption (top panel) and of TiO_2 particles (bottom panel) which generate the same radiative effect as the sulfate particles in the top panel (Pope et al., 2012) and which were used in the simulations shown in Fig. 6.

4 Conclusions and future work

Due to its high refractive index, TiO_2 has been highlighted as a possible alternative candidate particle to sulfuric acid (or its precursors) for injection into the stratosphere, where it would scatter solar radiation back into space as a solar radiation management scheme for the mitigation of global warming. However, the heterogeneous reactivity of TiO_2 towards stratospheric trace gases, e.g., N_2O_5 and $ClONO_2$, needs to be fully understood to assess the atmospheric chemistry consequences of such interventions. In this work for the first time, the heterogeneous reaction of N_2O_5 with airborne

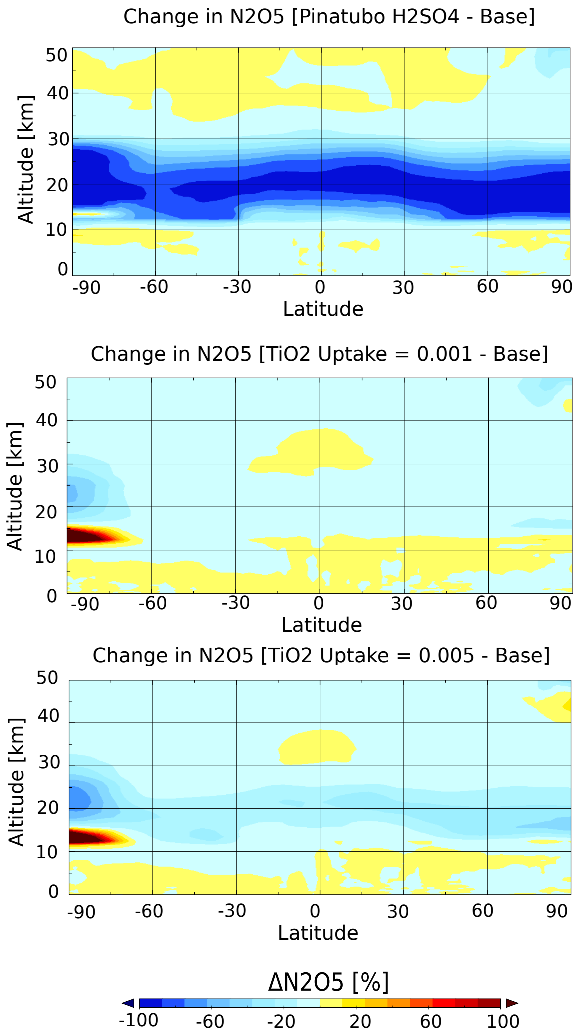

Figure 6. Simulated changes in N_2O_5 concentrations caused by Mt Pinatubo eruption (Top), and TiO_2 injection with $\gamma(N_2O_5)$ of 0.001 (middle) and 0.005 (bottom).

submicron TiO_2 particles has been investigated at room temperature and as a function of RH (up to 60 %). The uptake coefficient of N_2O_5 onto TiO_2 was determined to be $\sim 1.0 \times 10^{-3}$ at low RH. The increase to $\sim 3 \times 10^{-3}$ at 60 % RH, probably because of the formation of multilayers of surface-adsorbed water on TiO_2 particles, starts at 50–60 %. Uptake of N_2O_5 onto TiO_2 particles is relatively efficient, though much slower than that onto sulfuric acid particles.

To investigate the effect of these measurements we included the uptake of N_2O_5 onto TiO_2 particles in a simplistic experiment using the UKCA chemistry–climate model. We then studied the impact of introducing 10 Tg of TiO_2 into the stratosphere, which has been suggested to produce a radiative effect similar to that of the Mt Pinatubo eruption (Pope et al., 2012). We found, whilst the aerosols produced appreciable reductions in N_2O_5 concentration (up to 30 % depending on the uptake coefficient), they were significantly smaller in size and extent than those seen after the Mt Pinatubo eruption, where N_2O_5 depletion was over 90 % through much of the lower stratosphere.

The impact on ozone was also studied, with small increases (2–3 %) simulated throughout the stratosphere. These increases are similar to the middle stratospheric increases we found in our previous study of the Mt Pinatubo eruption, and here we do not calculate any lower stratospheric ozone reduction, which contrasts with the large depletions seen in the lower stratosphere after the Pinatubo eruption. This is the result of the omission of the activation of chlorine on TiO_2 particles in our simple experiment. Therefore, the heterogeneous reactions of TiO_2 with chlorine containing trace gases (e.g., $ClONO_2$, HOCl, and HCl) in the stratosphere need to be investigated before we can fully assess the impact of TiO_2 on stratospheric ozone. One previous study (Molina et al., 1997) investigated the uptake of $ClONO_2$ ($1–10 \times 10^{-7}$ Torr) onto aluminum oxide and Pyrex glass in the presence of HCl ($1–10 \times 10^{-6}$ Torr) at 210–220 K, and suggested that this process is very efficient, with an uptake coefficient of 0.02, which is > 10 times larger than that onto stratospheric sulfuric acid aerosols. In addition, the uptake of N_2O_5 onto HCl-doped sulfuric acid (Talukdar et al., 2012) and SiO_2 (Raff et al., 2009) leads to the formation of $ClNO_2$, whose photolysis will release Cl atoms and therefore represent a pathway for chlorine activation (Ghosh et al., 2012). Heterogeneous chlorine activation is not included in the modelling work because of the lack of reliable kinetics data. The uptake of $ClONO_2$ onto airborne mineral particles is under investigation in an ongoing study, and new laboratory data will be included in the model to assess the effect of heterogeneous chlorine activation on stratospheric O_3 in further work. Additionally, the potential photocatalytic activity of TiO_2 is likely to play a role. For example, the uptake of NO_2 on TiO_2 particles is enhanced under irradiation (Gustafsson et al., 2006; Ndour et al., 2008; El Zein and Bedjanian, 2012), leading to the formation of HONO, the photolysis of which produces NO and OH and may perturb the stratospheric NO_x and HO_x cycles. Heterogeneous chemical oxidation of SO_2 could enhance the formation of sulfate coating on mineral particles (Shang et al., 2010). Future studies will address this aspect.

Our simulations, which are designed to focus on chemistry effects, neglect feedbacks between the aerosol heating, the dynamics, and chemistry. However, the nudging has those feedbacks implicitly included for the volcanic aerosol case, which may or may not be a valid and good-enough assumption for TiO_2. Interactive feedbacks could also contribute to chemistry changes through factors such as the modification of the Quasi-Biennial Oscillation (Telford et al., 2009), strengthening of polar vortices (Thomas et al., 2009), and increasing uplift (Rosenfield et al., 1997). Our description of the aerosol particles is also simple; obviously particles with uniform radii distributed as the products of the Pinatubo eruption would be impossible to obtain. Variations in the distribution and radii of the particles will change the surface area density, and thus the chemical and optical impacts. To fully quantify the effects of the injection of any aerosol into the stratosphere a more complete simulation would be required.

Much consideration is required before any solar radiation management scheme could be considered. This will include feasiblility studies on the technical, political, social, and environmental feasibility of the scheme. One of the most important considerations is the effect of the scheme on the stratospheric chemistry and in particular the ozone layer. This work shows that the use of TiO_2 might offer benefits, when compared to sulfuric acid, by causing less perturbation to N_2O_5 chemistry, but further studies are required to fully understand the chemical consequences as discussed above.

Acknowledgements. We would like to thank J. Crowley and G. Schuster (Max Planck Institute for Chemistry, Germany) for providing us their initial design of the aerosol flow tube, and G. Bozóki (DuPont, Hungary) for offering us the FEPD suspension used to coat the flow tubes. This project was funded by EPSRC grant number EP/I01473X/1. The model simulations were performed on the HECToR computing facility. We acknowledge ECWMF and Paul Berrisford for the ERA-INTERIM analyses used to constrain the model.

Edited by: T. Bartels-Rausch

References

Al-Hosney, H. A. and Grassian, V. H.: Water, sulfur dioxide and nitric acid adsorption on calcium carbonate: A transmission and ATR-FTIR study, Phys. Chem. Chem. Phys., 7, 1266–1276, 2005.

Ammann, M., Cox, R. A., Crowley, J. N., Jenkin, M. E., Mellouki, A., Rossi, M. J., Troe, J., and Wallington, T. J.: Evaluated kinetic and photochemical data for atmospheric chemistry: Volume VI – heterogeneous reactions with liquid substrates, Atmos. Chem. Phys., 13, 8045–8228, doi:10.5194/acp-13-8045-2013, 2013.

Balkanski, Y., Schulz, M., Claquin, T., and Guibert, S.: Reevaluation of Mineral aerosol radiative forcings suggests a better agreement with satellite and AERONET data, Atmos. Chem. Phys., 7, 81–95, doi:10.5194/acp-7-81-2007, 2007.

Bedjanian, Y. and El Zein, A.: Interaction of NO_2 with TiO_2 Surface Under UV Irradiation: Products Study, J. Phys. Chem. A, 116, 1758–1764, doi:10.1021/jp210078b, 2012.

Bertram, T. H. and Thornton, J. A.: Toward a general parameterization of N_2O_5 reactivity on aqueous particles: the competing effects of particle liquid water, nitrate and chloride, Atmos. Chem. Phys., 9, 8351–8363, doi:10.5194/acp-9-8351-2009, 2009.

Braesicke, P., Abraham, N. L., Pyle, J. A., Yang, J., and Telford, P. J.: How well can we model polar spring ozone variability in a CCM?, Atmos. Chem. Phys. Discuss., in preparation, 2014.

Broadley, S. L., Murray, B. J., Herbert, R. J., Atkinson, J. D., Dobbie, S., Malkin, T. L., Condliffe, E., and Neve, L.: Immersion mode heterogeneous ice nucleation by an illite rich powder representative of atmospheric mineral dust, Atmos. Chem. Phys., 12, 287–307, doi:10.5194/acp-12-287-2012, 2012.

Brown, R. L.: Tubular flow reactors with first-order kinetics, J. Res. Nat. Bur. Stand., 83, 1–8, 1978.

Brown, S. S. and Stutz, J.: Nighttime radical observations and chemistry, Chem. Soc. Rev., 41, 6405–6447, doi:10.1039/c2cs35181a, 2012.

Brown, S. S., Ryerson, T. B., Wollny, A. G., Brock, C. A., Peltier, R., Sullivan, A. P., Weber, R. J., Dube, W. P., Trainer, M., Meagher, J. F., Fehsenfeld, F. C., and Ravishankara, A. R.: Variability in nocturnal nitrogen oxide processing and its role in regional air quality, Science, 311, 67–70, 2006.

Crowley, J. N., Ammann, M., Cox, R. A., Hynes, R. G., Jenkin, M. E., Mellouki, A., Rossi, M. J., Troe, J., and Wallington, T. J.: Evaluated kinetic and photochemical data for atmospheric chemistry: Volume V – heterogeneous reactions on solid substrates, Atmos. Chem. Phys., 10, 9059–9223, doi:10.5194/acp-10-9059-2010, 2010.

Crutzen, P. J.: Albedo enhancement by stratospheric sulfur injections: A contribution to resolve a policy dilemma?, Clim. Change, 77, 211–219, doi:10.1007/s10584-006-9101-y, 2006.

Cziczo, D. J., Froyd, K. D., Hoose, C., Jensen, E. J., Diao, M., Zondlo, M. A., Smith, J. B., Twohy, C. H., and Murphy, D. M.: Clarifying the Dominant Sources and Mechanisms of Cirrus Cloud Formation, Science, 340, 1320–1324, doi:10.1126/science.1234145, 2013.

Dee, D. P., Uppala, S. M., Simmons, A. J., Berrisford, P., Poli, P., Kobayashi, S., Andrae, U., Balmaseda, M. A., Balsamo, G., Bauer, P., Bechtold, P., Beljaars, A. C. M., van de Berg, L., Bidlot, J., Bormann, N., Delsol, C., Dragani, R., Fuentes, M., Geer, A. J., Haimberger, L., Healy, S. B., Hersbach, H., Holm, E. V., Isaksen, L., Kallberg, P., Kohler, M., Matricardi, M., McNally, A. P., Monge-Sanz, B. M., Morcrette, J. J., Park, B. K., Peubey, C., de Rosnay, P., Tavolato, C., Thepaut, J. N., and Vitart, F.: The ERA-Interim reanalysis: configuration and performance of the data assimilation system, Q. J. Roy. Meteor. Soc., 137, 553–597, doi:10.1002/qj.828, 2011.

Dentener, F. J. and Crutzen, P. J.: Reaction of N_2O_5 on Tropospheric Aerosols – Impact on the Global Distributions of NO_x, O_3, and OH, J. Geophys. Res.-Atmos., 98, 7149–7163, 1993.

Dentener, F. J., Carmichael, G. R., Zhang, Y., Lelieveld, J., and Crutzen, P. J.: Role of mineral aerosol as a reactive surface in the global troposphere, J. Geophys. Res.-Atmos., 101, 22869–22889, 1996.

Dutton, E. G. and Christy, J. R.: Solar radiative forcing at selected locations and evidence for global lower tropospheric cooling following the eruption of El-Ehichon and Pinatubo, Geophys. Res. Lett., 19, 2313–2316, doi:10.1029/92gl02495, 1992.

El Zein, A. and Bedjanian, Y.: Interaction of NO_2 with TiO_2 surface under UV irradiation: measurements of the uptake coefficient, Atmos. Chem. Phys., 12, 1013–1020, doi:10.5194/acp-12-1013-2012, 2012.

Fahey, D. W., Eubank, C. S., Hubler, G., and Fehsenfeld, F. C.: A Calibrated Source of N_2O_5, Atmos. Environ., 19, 1883–1890, 1985.

Fahey, D. W., Kawa, S. R., Woodbridge, E. L., Tin, P., Wilson, J. C., Jonsson, H. H., Dye, J. E., Baumgardner, D., Borrmann, S., Toohey, D. W., Avallone, L. M., Proffitt, M. H., Margitan, J., Loewenstein, M., Podolske, J. R., Salawitch, R. J., Wofsy, S. C., Ko, M. K. W., Anderson, D. E., Schoeberl, M. R., and Chan, K. R.: In situ measuremnet constraining the role of sulfate aerosol in midelatitude ozone depletion, Nature, 363, 509–514, doi:10.1038/363509a0, 1993.

Ferraro, A. J., Highwood, E. J., and Charlton-Perez, A. J.: Stratospheric heating by potential geoengineering aerosols, Geophys. Res. Lett., 38, L24706, doi:10.1029/2011gl049761, 2011.

Fuchs, N. A. and Sutugin, A. G.: Highly dispersed aerosols, Ann Arbor Sci., Ann Arbor, chapter 3, p. 46, 1970.

Ghosh, B., Papanastasiou, D. K., Talukdar, R. K., Roberts, J. M., and Burkholder, J. B.: Nitryl Chloride (ClNO2): UV/Vis Absorption Spectrum between 210 and 296 K and O(P-3) Quantum Yield at 193 and 248 nm, J. Phys. Chem. A, 116, 5796–5805, doi:10.1021/jp207389y, 2012.

Goodman, A. L., Bernard, E. T., and Grassian, V. H.: Spectroscopic study of nitric acid and water adsorption on oxide particles: Enhanced nitric acid uptake kinetics in the presence of adsorbed water, J. Phys. Chem. A, 105, 6443–6457, 2001.

Griffiths, P. T., Badger, C. L., Cox, R. A., Folkers, M., Henk, H. H., and Mentel, T. F.: Reactive Uptake of N_2O_5 by Aerosols Containing Dicarboxylic Acids. Effect of Particle Phase, Composition, and Nitrate Content, J. Phys. Chem. A, 113, 5082–5090, doi:10.1021/jp8096814, 2009.

Guo, S., Bluth, G. J. S., Rose, W. I., Watson, I. M., and Prata, A. J.: Re-evaluation of SO_2 release of the 15 June 1991 Pinatubo eruption using ultraviolet and infrared satellite sensors, Geochem. Geophy. Geosy., 5, Q04001, doi:10.1029/2003gc000654, 2004.

Gustafsson, R. J., Orlov, A., Griffiths, P. T., Cox, R. A., and Lambert, R. M.: Reduction of NO_2 to nitrous acid on illuminated titanium dioxide aerosol surfaces: implications for photocatalysis and atmospheric chemistry, Chem. Commun., 9, 3936–3938, 2006.

Hanisch, F. and Crowley, J. N.: Ozone decomposition on Saharan dust: an experimental investigation, Atmos. Chem. Phys., 3, 119–130, doi:10.5194/acp-3-119-2003, 2003.

Hanson, D. R. and Ravishankara, A. R.: The reaction probabilities of $ClONO_2$ and N_2O_5 on polar stratospheric cloud materials, J. Geophys. Res.-Atmos., 96, 5081–5090, 1991.

Hatch, C. D., Wiese, J. S., Crane, C. C., Harris, K. J., Kloss, H. G., and Baltrusaitis, J.: Water Adsorption on Clay Minerals As a Function of Relative Humidity: Application of BET and Freundlich Adsorption Models, Langmuir, 28, 1790–1803, doi:10.1021/la2042873, 2011.

Hinds, W. C.: Aerosol techniques: properties, behavior, and measurement if airborne particles, John Wiley & Sons. Inc., New York, 1996.

Houston, P. L.: Chemical Kinetics and Reaction Dynamics, McGraw-Hill, Dubuque and Boston, 2001.

Huneeus, N., Schulz, M., Balkanski, Y., Griesfeller, J., Prospero, J., Kinne, S., Bauer, S., Boucher, O., Chin, M., Dentener, F., Diehl, T., Easter, R., Fillmore, D., Ghan, S., Ginoux, P., Grini, A., Horowitz, L., Koch, D., Krol, M. C., Landing, W., Liu, X., Mahowald, N., Miller, R., Morcrette, J.-J., Myhre, G., Penner, J., Perlwitz, J., Stier, P., Takemura, T., and Zender, C. S.: Global dust model intercomparison in AeroCom phase I, Atmos. Chem. Phys., 11, 7781–7816, doi:10.5194/acp-11-7781-2011, 2011.

Karagulian, F., Santschi, C., and Rossi, M. J.: The heterogeneous chemical kinetics of N_2O_5 on $CaCO_3$ and other atmospheric mineral dust surrogates, Atmos. Chem. Phys., 6, 1373–1388, doi:10.5194/acp-6-1373-2006, 2006.

Keyser, L. F.: High-Pressure Flow Kinetics – a Study of the OH + HCl Reaction from 2 to 100 Torr, J. Phys. Chem., 88, 4750–4758, 1984.

Linsebigler, A. L., Lu, G., and Yates, J. T.: Photocatalysis on TiO_2 Surfaces: Principles, Mechanisms, and Selected Results, Chem. Rev., 95, 735–758, doi:10.1021/cr00035a013, 1995.

McCormick, M. P., Thomason, L. W., and Trepte, C. R.: Atmospheric effects of the Mt Pinatubo eruption, Nature, 373, 399–404, doi:10.1038/373399a0, 1995.

McNeill, V. F., Patterson, J., Wolfe, G. M., and Thornton, J. A.: The effect of varying levels of surfactant on the reactive uptake of N_2O_5 to aqueous aerosol, Atmos. Chem. Phys., 6, 1635–1644, doi:10.5194/acp-6-1635-2006, 2006.

Mogili, P. K., Kleiber, P. D., Young, M. A., and Grassian, V. H.: N_2O_5 hydrolysis on the components of mineral dust and sea salt aerosol: Comparison study in an environmental aerosol reaction chamber, Atmos. Environ., 40, 7401–7408, 2006.

Molina, M. J., Molina, L. T., and Kolb, C. E.: Gas-phase and heterogeneous chemical kinetics of the troposphere and stratosphere, Annu. Rev. Phys. Chem., 47, 327–367, 1996.

Molina, M. J., Molina, L. T., Zhang, R. Y., Meads, R. F., and Spencer, D. D.: The reaction of $ClONO_2$ with HCl on aluminum oxide, Geophys. Res. Lett., 24, 1619–1622, doi:10.1029/97gl01560, 1997.

Morgenstern, O., Braesicke, P., O'Connor, F. M., Bushell, A. C., Johnson, C. E., Osprey, S. M., and Pyle, J. A.: Evaluation of the new UKCA climate-composition model – Part 1: The stratosphere, Geosci. Model Dev., 2, 43–57, doi:10.5194/gmd-2-43-2009, 2009.

Nakata, K. and Fujishima, A.: TiO_2 photocatalysis: Design and applications, J. Photoch. Photobio. C, 13, 169–189, 2012.

Ndour, M., D'Anna, B., George, C., Ka, O., Balkanski, Y., Kleffmann, J., Stemmler, K., and Ammann, M.: Photoenhanced uptake of NO_2 on mineral dust: Laboratory experiments and model simulations, Geophys. Res. Lett., 35, L05812, doi:10.1029/2007gl032006, 2008.

Nicolas, M., Ndour, M., Ka, O., D'anna, B., and George, C.: Photochemistry of atmospheric dust: ozone decomposition on illuminatd titanium dioxide, Environ. Sci. Technol., 43, 7347–7442, 2009.

O'Connor, F. M., Johnson, C. E., Morgenstern, O., Abraham, N. L., Braesicke, P., Dalvi, M., Folberth, G. A., Sanderson, M. G., Telford, P. J., Voulgarakis, A., Young, P. J., Zeng, G., Collins, W. J., and Pyle, J. A.: Evaluation of the new UKCA climate-composition model – Part 2: The Troposphere, Geosci. Model Dev., 7, 41–91, doi:10.5194/gmd-7-41-2014, 2014.

Phillips, G. J., Tang, M. J., Thieser, J., Brickwedde, B., Schuster, G., Bohn, B., Lelieveld, J., and Crowley, J. N.: Significant concentrations of nitryl chloride observed in rural continental Europe associated with the influence of sea salt chloride and anthropogenic emissions, Geophys. Res. Lett., 39, L10811, doi:10.1029/2012gl051912, 2012.

Pope, F. D., Braesicke, P., Grainger, R. G., Kalberer, M., Watson, I. M., Davidson, P. J., and Cox, R. A.: Stratospheric aerosol particles and solar-radiation management, Nature Clim. Change, 2, 713–719, 2012.

Pöschl, U., Rudich, Y., and Ammann, M.: Kinetic model framework for aerosol and cloud surface chemistry and gas-particle interactions – Part 1: General equations, parameters, and terminology, Atmos. Chem. Phys., 7, 5989–6023, doi:10.5194/acp-7-5989-2007, 2007.

Pradhan, M., Kalberer, M., Griffiths, P. T., Braban, C. F., Pope, F. D., Cox, R. A., and Lambert, R. M.: Uptake of Gaseous Hydrogen Peroxide by Submicrometer Titanium Dioxide Aerosol as a Function of Relative Humidity, Environ. Sci. Technol., 44, 1360–1365, doi:10.1021/es902916f, 2010.

Raff, J. D., Njegic, B., Chang, W. L., Gordon, M. S., Dabdub, D., Gerber, R. B., and Finlaysonpitts, B. J.: Chrorine activation indoors and outdoors via surface-mediated reactions of nitrogen oxides with hydrogen chloride, P. Natl. Acad. Sci. USA, 106, 13647–13654, 2009.

Rosenfield, J. E., Considine, D. B., Meade, P. E., Bacmeister, J. T., Jackman, C. H., and Schoeberl, M. R.: Stratospheric effects of Mount Pinatubo aerosol studied with a coupled two-dimensional model, J. Geophys. Res.-Atmos., 102, 3649–3670, doi:10.1029/96jd03820, 1997.

Rouviere, A., Sosedova, Y., and Ammann, M.: Uptake of Ozone to Deliquesced KI and Mixed KI/NaCl Aerosol Particles, J. Phys. Chem. A, 114, 7085–7093, doi:10.1021/jp103257d, 2010.

Sander, S. P., Abbatt, J. P. D., Barker, J. R., Burkholder, J. B., Friedl, R. R., Golden, D. M., Huie, R. E., Kolb, C. E., Kurylo, M. J., Moortgat, G. K., Orkin, V. L., and Wine, P. H.: Chemical Kinetics and Photochemical Data for Use in Atmospheric Studies, Evaluation No. 17, JPL Publication 10-6, Jet Propulsion Lab., Pasadena, CA, 2011.

Sassine, M., Burel, L., D'Anna, B., and George, C.: Kinetics of the tropospheric formaldehyde loss onto mineral dust and urban surfaces, Atmos. Environ., 44, 5468–5475, 2010.

Seisel, S., Börensen, C., Vogt, R., and Zellner, R.: Kinetics and mechanism of the uptake of N_2O_5 on mineral dust at 298 K, Atmos. Chem. Phys., 5, 3423–3432, doi:10.5194/acp-5-3423-2005, 2005.

Shang, J., Li, J., and Zhu, T.: Heterogeneous reaction of SO_2 on TiO_2 particles, Sci. China Chem., 53, 2637–2643, doi:10.1007/s11426-010-4160-3, 2010.

Shepherd, J.: Geoengineering the climate: science, governance and uncertainty, The Royal Society, 2009.

Solomon, S.: Stratospheric ozone depletion: A review of concepts and history, Rev. Geophys., 37, 275–316, 1999.

SPARC: Assessment of Stratospheric Aerosol Properties (SPARCR Report No. 4), 2006.

Sullivan, R. C., Guazzotti, S. A., Sodeman, D. A., and Prather, K. A.: Direct observations of the atmospheric processing of Asian mineral dust, Atmos. Chem. Phys., 7, 1213–1236, doi:10.5194/acp-7-1213-2007, 2007.

Talukdar, R. K., Burkholder, J. B., Roberts, J. M., Portmann, R. W., and Ravishankara, A. R.: Heterogeneous Interaction of N_2O_5 with HCl Doped H_2SO_4 under Stratospheric Conditions: $ClNO_2$ and Cl-2 Yields, J. Phys. Chem. A, 116, 6003–6014, doi:10.1021/jp210960z, 2012.

Tang, M. J., Thieser, J., Schuster, G., and Crowley, J. N.: Uptake of NO_3 and N_2O_5 to Saharan dust, ambient urban aerosol and soot: a relative rate study, Atmos. Chem. Phys., 10, 2965–2974, doi:10.5194/acp-10-2965-2010, 2010.

Tang, M. J., Thieser, J., Schuster, G., and Crowley, J. N.: Kinetics and mechanism of the heterogeneous reaction of N_2O_5 with mineral dust particles, Phys. Chem. Chem. Phys., 14, 8551–8561, doi:10.1039/c2cp40805h, 2012.

Tang, M. J., Schuster, G., and Crowley, J. N.: Heterogeneous reaction of N_2O_5 with illite and Arizona test dust particles, Atmos. Chem. Phys., 14, 245–254, doi:10.5194/acp-14-245-2014, 2014.

Telford, P. J., Braesicke, P., Morgenstern, O., and Pyle, J. A.: Technical Note: Description and assessment of a nudged version of the new dynamics Unified Model, Atmos. Chem. Phys., 8, 1701–1712, doi:10.5194/acp-8-1701-2008, 2008.

Telford, P. J., Braesicke, P., Morgenstern, O., and Pyle, J.: Reassessment of causes of ozone column variability following the eruption of Mount Pinatubo using a nudged CCM, Atmos. Chem. Phys., 9, 4251–4260, doi:10.5194/acp-9-4251-2009, 2009.

Telford, P. J., Abraham, N. L., Archibald, A. T., Braesicke, P., Dalvi, M., Morgenstern, O., O'Connor, F. M., Richards, N. A. D., and Pyle, J. A.: Implementation of the Fast-JX Photolysis scheme (v6.4) into the UKCA component of the MetUM chemistry-climate model (v7.3), Geosci. Model Dev., 6, 161–177, doi:10.5194/gmd-6-161-2013, 2013.

Telford, P. J., Archibald, A. T., Abraham, N. L., Braesicke, P., Dalvi, M., Johnson, C., Keeble, J., O'Connor, F., Squire, O., and Pyle, J. A.: Evaluation of the UM-UKCA model configuration for Chem- istry of the Stratosphere and Troposphere (CheST), Geosci. Model Dev. Discuss., in preparation, 2014.

Textor, C., Schulz, M., Guibert, S., Kinne, S., Balkanski, Y., Bauer, S., Berntsen, T., Berglen, T., Boucher, O., Chin, M., Dentener, F., Diehl, T., Easter, R., Feichter, H., Fillmore, D., Ghan, S., Ginoux, P., Gong, S., Grini, A., Hendricks, J., Horowitz, L., Huang, P., Isaksen, I., Iversen, I., Kloster, S., Koch, D., Kirkevåg, A., Kristjansson, J. E., Krol, M., Lauer, A., Lamarque, J. F., Liu, X., Montanaro, V., Myhre, G., Penner, J., Pitari, G., Reddy, S., Seland, Ø., Stier, P., Takemura, T., and Tie, X.: Analysis and quantification of the diversities of aerosol life cycles within AeroCom, Atmos. Chem. Phys., 6, 1777–1813, doi:10.5194/acp-6-1777-2006, 2006.

Thomas, M. A., Timmreck, C., Giorgetta, M. A., Graf, H.-F., and Stenchikov, G.: Simulation of the climate impact of Mt. Pinatubo eruption using ECHAM5 – Part 1: Sensitivity to the modes of atmospheric circulation and boundary conditions, Atmos. Chem. Phys., 9, 757–769, doi:10.5194/acp-9-757-2009, 2009.

Thornton, J. A., Braban, C. F., and Abbatt, J. P. D.: N_2O_5 hydrolysis on sub-micron organic aerosols: the effect of relative humidity, particle phase, and particle size, Phys. Chem. Chem. Phys., 5, 4593–4603, 2003.

Thornton, J. A., Kercher, J. P., Riedel, T. P., Wagner, N. L., Cozic, J., Holloway, J., S., Dube, W. P., Wolfe, G. M., Quinn, P. K., Middlebrook, A. M., Alexander, B., and Brown, S. S.: A large atomic chlorine source inferred from mid-continental reactive nitrogen chemistry, Nature, 464, 271–174, 2010.

Tilmes, S., Muller, R., and Salawitch, R.: The sensitivity of polar ozone depletion to proposed geoengineering schemes, Science, 320, 1201–1204, doi:10.1126/science.1153966, 2008.

Usher, C. R., Michel, A. E., and Grassian, V. H.: Reactions on mineral dust, Chem. Rev., 103, 4883–4939, 2003.

Wagner, C., Hanisch, F., Holmes, N., de Coninck, H., Schuster, G., and Crowley, J. N.: The interaction of N_2O_5 with mineral dust: aerosol flow tube and Knudsen reactor studies, Atmos. Chem. Phys., 8, 91–109, doi:10.5194/acp-8-91-2008, 2008.

Wagner, C., Schuster, G., and Crowley, J. N.: An aerosol flow tube study of the interaction of N_2O_5 with calcite, Arizona dust and quartz, Atmos. Environ., 43, 5001–5008, 2009.

Wayne, R. P., Barnes, I., Biggs, P., Burrows, J. P., Canosamas, C. E., Hjorth, J., Lebras, G., Moortgat, G. K., Perner, D., Poulet, G., Restelli, G., and Sidebottom, H.: The nitrate radical-physics, chemistry, and the atmosphere, Atmos. Environ. A-Gen., 25, 1–203, 1991.